6-2016

Constraining Cosmological Parameters Using the Correlation Function

Michael Warrener
Union College - Schenectady, NY

Constraining Cosmological Parameters Using The Correlation Function

By

Michael Jacob Warrener

* * * * * * * * *

Submitted in partial fulfillment

of the requirements for

Honors in the Department of Physics and Astronomy

UNION COLLEGE

May, 2016

ABSTRACT

WARRENER, MICHAEL Constraining Cosmological Parameters Using the Correlation Function

ADVISOR: Jonathan Marr

As the European Space Agency prepares to launch the space telescope Euclid in 2020, we are interested in using its observations of galaxy clustering as a new geometry-based tool to constrain the cosmological parameters Ω_M and Ω_Λ. In this work, we use data simulated by *Magneticum* (a high-resolution cosmological structure simulation) to model the correlation functions of both galaxies and clusters at several redshifts. We fit analytic models to the simulated data centered at the baryon acoustic oscillation peak to extract both the matter density parameter Ω_M and the dark energy density parameter Ω_Λ. We find that the correct cosmology is within the 68% confidence interval for both galaxies and clusters of galaxies.

Contents

1 Introduction

Since the onset of modern cosmology, with Hubble's discovery of the expansion of the universe (Hubble 1929), astronomers have sought to determine both the origin and fate of the universe. By correlating the distance to a particular galaxy to its recessional velocity, Hubble derived a linear relation $v = H_0 d$, where H_0, the Hubble Constant, had a value of 550 $km/s/Mpc$. Today, we measure the Hubble Constant to actually be 70.4 $km/s/Mpc$, as shown in Table 1. Hubble's relationship was true regardless of direction and implied one of two things: either we are at the very center of the universe, or space itself is expanding, thus moving everything away from everything else. Originally differentiated by the Copernican Principle (which states that we are not special) then later by observations, Hubble concluded that space itself must be expanding. This led to the Big Bang Theory, in which the universe had a beginning, since extrapolating backwards in time leads to a situation in which all matter is together (Alpher, Bethe, & Gamow 1948). An alternative model, the Steady State Theory, in which matter is created as the universe expands, competed for a while but was disproved in 1964 with the discovery of the relic radiation left over from the hot early universe (Penzias & Wilson 1965). With an evolving universe, the question arose as to what the universe looked like in the past. Earlier work by Alexander Friedmann (1922) revealed that in order to study the evolution of the universe, its composition and structure must be known.

Instead of talking about the composition of the universe in absolute terms like total energy, or even density, we use a parameter Ω, which is the ratio of the actual density to the *critical density*. In the early days of modern cosmology, before the discovery in 1998 that the universe's expansion is accelerating, the critical density was defined as the density at which the universe would recollapse under its own gravity. The case of the increase in the universe's expansion rate is not, at this time, known, but it requires an additional energy term, which is referred to as *dark energy*,

or Λ. In order to make it easier to measure Ω, it is decomposed into the constituent components of the universe, namely $\Omega_M, \Omega_\Lambda,$ & Ω_{rad}, the matter density, the dark energy density, and the radiation density, respectively. Ω_M includes both baryonic matter, which makes up all visible matter (gas, stars, and galaxies) and dark matter, which is composed of a currently undetected particle. The total Ω_M is dominated ($\sim 80\%$) by dark matter. By the Friedmann Equations, knowing these values makes it possible to understand the entire large-scale history of the universe from inception to any time in the future.

To quantify the composition of the universe, we can utilize the structure formed by the matter. One fundamental assumption in cosmology concerning the structure is that the universe is homogeneous and isotropic, that is, at large enough scales, there is no preferred direction or position to space, as initially shown by Hubble's observations. This assumption was supported by observations of the *cosmic microwave background* in 1964 by Penzias and Wilson (Penzias & Wilson 1965), which showed that the universe is awash in a $\sim 2.7\ K$ background thermal radiation field. This background is the relic of high-energy photons in the early universe. However, as the universe expanded, the wavelengths of the photons were stretched as space expanded, thus shifting the high-energy photons to lower energy over time. As observations improved, astronomers noticed that the background varied on the order of $10^{-4}\ K$ (Mather et al. 1990). Although small, these large-scale fluctuations added one more question to an already significant list of critical questions still open in cosmology: How can the universe both have structure and follow the cosmological principle, and why does the universe appear to be so close to being perfectly geometrically flat ($\Omega = 1$)?

In 1981, Alan Guth developed a new theory: *inflation*, which gave answers to all of these questions (Guth 1981). Inflation posits that during a very early time of the universe ($t = 10^{-36}$ to $t \approx 10^{-32}$ seconds), when the universe was around $10^{16}K$, the entirety of existence underwent a moment of extreme exponential expansion multi-

plying the size of the universe by a factor of about 10^{50}. This explosion of space-time expanded geometric distortions to such scales that the universe became everywhere homogeneous, isotropic, and flat, i.e. $\Omega = 1$ (Ryden 2002). For example, the degree of curvature κ of a circle is simply given by

$$\kappa = \frac{1}{r},$$

where r is the radius of the circle. So, a circle of unit radius which underwent inflation would go from curvature $\kappa = 1 \rightarrow \kappa = 10^{-50}$, which is well below current sensitivity. So, this circle would, for all practical purposes, appear to be flat. In three dimensions, this also explains how the universe is homogeneous and isotropic. To understand how structure arises, however, we will invoke quantum mechanics in the next section.

1.1 Baryon Acoustic Oscillations

One of the peculiarities of quantum mechanics is the notion that infinitesimal fluctuations in the energy profile (or field) of some sample of space must occur over sufficiently small time scales as quantified in the Heisenberg Uncertainty Principle. Normally, these fluctuations are so small that they are absolutely negligible. However, in the very early universe, these fluctuations caused microscopic perturbations in the density profile of all matter (and light, in fact), which expanded by about 50 e-foldings during the inflation epoch. These seemingly negligible inhomogeneities became large enough in size to create significant gravity wells.

During this time, all electrons were free (unbound to any atom) and could interact with all wavelengths of light because tcould undergo any change of energy. Thus, the baryonic matter was *coupled* to the photons. This coupling caused the baryonic matter profile to exactly reflect that of the photon profile. So, even though the baryonic matter attempted to collapse into the local gravity wells, the radiation

pressure (caused by the ten billion to one photon to baryon ratio) completely dwarfed the gravitational force, thus arresting the collapse. This did, however, create acoustic waves in the baryonic matter density profile, otherwise known as *baryon acoustic oscillations* (BAOs). Moreover, dark matter, which contributes significantly more mass than baryons, is presumed not to interact with with photons, so it was free to collapse into the potential wells, thus forming increasingly larger gravitational potentials centered on the initial perturbations.

At around 378,000 years after the Big Bang, the baryons had finally cooled enough for neutral hydrogen to form—an epoch known as *Recombination*. After the electrons became bound, they could only interact with light at very specific wavelengths (another effect of quantum mechanics), thus *decoupling* the light and baryonic matter. As there were now much fewer photon-baryon interactions, there was no longer any opposition to gravitational collapse. Thus, the matter could now collapse into the huge gravity wells created by the dark matter, which is why, we suspect, ordered structures appeared so quickly after Recombination. These regions resulted both from the initial quantum fluctuations and the acoustic waves. Simple expansion calculations predict that these gravity wells, and thus the resulting structures, would have a preferential separation distance equal to the *horizon size* at Recombination. This separation corresponds to approximately 105 Mpc/h today (or approximately 1° on the cosmic microwave background), where $h = \frac{H_0}{100\ km/s/Mpc}$ and H_0 is the current value of the Hubble Parameter (Peebles & Yu 1970).

The horizon size is a measure of the furthest space-time distance that an event could influence in the history of the universe to that time. Propagation of information is limited to the speed of light, and so for some given time interval, there is a characteristic distance that the information could travel. In a simplistic, flat, static universe, this would be simply $d = ct_0$, where c is the speed of light and t_0 is the age of the universe. In an expanding universe, the horizon size is larger because the light

traveled at the same speed when the universe was small and so traveled distances that, today, are much larger. For example, we expect that the during the epoch of Recombination, the horizon size is dictated by $d = 3ct_0$. Although our universe is neither simplistic nor static, this method nonetheless provides a measure of the largest influence that the dark matter gravity wells could have by Recombination.

1.2 The Two-Point Correlation Function

In order to utilize the theory of BAOs, we can use a statistical tool known as the *two-point correlation function* (Peebles 1980). The correlation function is applied to discrete distributions and measures the excess probability of finding an object at a given distance from another object. In its simplest form, the correlation function is

$$\xi(r)dr = \frac{DD(r)dr - RR(r)dr}{RR(r)dr} \tag{1}$$

where $DD(r)dr$ is the number of pairs of objects in the distribution which are separated by a distance between r and rdr and $RR(r)dr$ is the number of pairs of objects in a random sample separated between r and rdr. For example, if there are no over densities, then DD=RR, and $\xi(r)dr = 0$ meaning that there is no preference in the collection to be separated by a distance r.

The exact form of the correlation function that we use is from Landy & Szalay (1993)

$$\xi(r)dr = \frac{DD(r)dr}{RR(r)dr}\left(\frac{n_R}{n_D}\right)^2 - 2\frac{DR(r)dr}{RR(r)dr}\left(\frac{n_R}{n_D}\right) + 1 \tag{2}$$

where $DD(r)dr$ and $RR(r)dr$ are defined as above, n_D & n_R are the mean number densities of the data and random sample, respectively, and $DR(r)dr$ is the number of pairs of objects that are separated by a distance between r and rdr between the two catalogues.

We can compile a list of ξ for a set of separation distances, thus allowing us to

create a profile of the over density probability. When applied to observations of low redshift galaxies ($0 \leq z \leq 0.47$), a preferential separation distance around 105 Mpc/h is, in fact, found (Eisenstein et al. 2005; and citations therein).

It has been shown that the precise location of the BAO peak in the $\xi(r)$ profile is directly related to the values of the cosmological parameters, which we will explore in the next section (Eisenstein et al. 2005). Depending on the values of specific cosmological parameters, the inferred length scale of the peak in the correlation function shifts ever so slightly to larger or smaller separation distances. This length scale is affected by the dark matter quantity, the amount of dark energy, as indicated by the value of Λ, the amount of baryonic matter, and the Hubble Constant. In this work, we assume that the baryonic matter density is well-determined, and we leave all results in units of Mpc/h, so we need not assume a value for the Hubble constant. Therefore, we seek to use the BAO peak in the correlation function to measure Ω_M and Ω_Λ.

1.3 The Comoving Volume Distance

In compliment to the results of luminosity-based methods (such as using Type Ia supernova (Riess et al. 1998)), the BAO peak can be a very powerful geometry-based tool in constraining many fundamental parameters in cosmology (Blake & Glazebrook 2003). Unlike measurements of Type Ia supernova, which use the concept of a *standard candle* (in which the intrinsic brightness of the object is assumed and distance is thus calculated), the BAO acts as a *standard ruler*. Here, we know the physical size of an object, and thus infer the distance using geometric arguments.

In order to infer the distance, however, some measure of distance must be agreed upon. Here, we use a distance derived from the *differential comoving volume*, which is defined as follows

$$dV_c = \frac{c}{H_0} \frac{(1+z)^2 D_A^2(z)}{E(z)} d\Omega dz \tag{3}$$

where H_0 is the Hubble Constant, z is the redshift, D_A is the angular diameter distance, Ω is a solid-angle, and $E(z)$ is a dimensionless factor containing the z-dependence of $H(z)$, i.e. $H(z) = H_0 E(z)$, where $H(z)$ is the Hubble Parameter (Hogg 2000). Following Peebles, p. 319, (1993) D_A is defined by equating an object's angular size on the sky (in radians) to the ratio of its physical length to its distance, and, in the case of a flat universe, is given by

$$D_A = \frac{D_p}{1+z} \tag{4}$$

where D_p is the proper distance given by the Robertson-Walker Metric as

$$D_p = a_0 \int_{t_e}^{t_0} \frac{c}{a(t)} dt \tag{5}$$

where a_0 is the current scale factor of the universe, t_e is the time when the tracer photon was emitted, and t_0 is the current age of the universe. We can change to an integration over scale factor a by realizing

$$dt = \frac{da}{\dot{a}}. \tag{6}$$

So,

$$D_A = \frac{a_0}{1+z} \int_{a(t_e)}^{a_0} \frac{c}{a\dot{a}} da. \tag{7}$$

Using $H \equiv \dot{a}/a$, this may be written as

$$D_A = \frac{a_0}{1+z} \int_{a(t_e)}^{a_0} \frac{c}{Ha^2} da. \tag{8}$$

Having simplified our expression this far, it is helpful to convert into a function of

redshift z instead of a. We can do this by using the basic cosmological relation

$$\frac{a_0}{a} \equiv 1 + z. \tag{9}$$

So

$$\frac{da}{a_0} = \frac{-dz}{(1+z)^2} \tag{10}$$

$$da = -\frac{a^2}{a_0} dz. \tag{11}$$

Substituting in for da, we find

$$D_A = \frac{a_0}{1+z} \int_z^0 -\frac{c}{Ha^2} \frac{a^2}{a_0} dz'. \tag{12}$$

Using the fact that $H(z) = H_0 E(z)$, and simplifying the above equation, we find

$$D_A = \frac{c/H_0}{1+z} \int_0^z \frac{dz'}{E(z')}. \tag{13}$$

The function $E(z)$, which contains the z-dependence of H, also depends on Ω_M and Ω_Λ can be found any introductory cosmology text (such as Ryden (2002)) and is given by

$$E(z) = \sqrt{\Omega_M (1+z)^3 + (1 - \Omega_M - \Omega_\Lambda)(1+z)^2 + \Omega_\Lambda}. \tag{14}$$

Thus, as dV_c is a function of both D_A and $E(z)$, which both depend on Ω_M and Ω_Λ, we see that the differential comoving volume is itself fundamentally a function of Ω_M and Ω_Λ.

We can define a "distance" scale by considering $\frac{dV_c}{dz d\Omega}$. Taking the cube root of this yields a Comoving Volume Distance D_V that can be used to define an internal

measurement.

$$D_V = \left(\frac{c}{H_0} \frac{(1+z)^2 D_A^2(z)}{E(z)} \right)^{1/3}. \tag{15}$$

This is a spherically averaged distance measure, so it incorporates all three dimensions of space, which is the case with observational data.

By creating a set of D_V values at specified redshifts, we can find $(\Omega_M, \Omega_\Lambda)$ satisfying Equation 15, and thus, observations of galaxy distributions can be related back to the cosmological parameters. Such a distribution is one of the many capacities of the European Space Agency's telescope *Euclid* set to launch in 2020. Thus, we seek to finalize the analysis method in time for the telescope's launch.

2 Methods

2.1 Sample Preparation

In order to create the simulated observations, we used a program known as *Magneticum*, a high-resolution, entropy-conserving, smooth particle hydrodynamic (SPH) simulation covering about $0.7(Gpc/h)^3$ using WMAP7 cosmology as given in Table 1[1]. *Magneticum* is based on GADGET-3 (Springel et al. 2005) and incorporates a low-viscosity SPH regime to track turbulence (Dolag et al. 2005). The simulation begins at $z = 120$ when the universe is still very smooth, and so the power spectrum is linear (Dolag in prep).

We calculated the correlation function from the *Magneticum* output at four redshifts: 0.20, 0.52, 0.72, & 1.00. This required us to choose a spatial resolution for our analysis. It was important to make the spatial resolution fine enough to see the morphological features in question but no smaller. If the resolution was too fine, the errors in the correlation function were so large than no meaningful data could be

[1] `http://www.magneticum.org/simulations.html`

extracted. If it were too coarse, we could not constrain significantly the location of the BAO peak in the correlation function.

We also reduced the errors in the analysis using a technique called *jackknife,* wherein we subdivided the sample volume into a number N of spatial cubes called *mocks*. We calculated the correlation function for all of the data less one mock, then averaged over all N of these partial correlation functions. This method dramatically decreased the uncertainties in the correlation function with greater decrease as the number of mocks increased. The limiting factor on the number of mocks was computational time as more mocks required more calculations of the correlation function.

2.2 Fitting the Correlation Function

In order to fit the cosmological parameters, we compared the simulation data to two theoretical distributions using the Code for Anisotropies in the Microwave Background (CAMB) (Lewis & Bridle 2002) and a pre-BAO model from Eisenstein and Hu (Eisenstein & Hu 1998). These are independent codes designed to calculate the power spectrum at a given redshift in different ways. The Eisenstein-Hu (EH) model is formulated without a BAO peak, and thus we include it as a control. Unlike *Magneticum*, which evolves a system using some assumed cosmology, these models calculate the correlation function, which is the Fourier transform of the power spectrum, using a theoretical evolution model. The correlation functions of these models were then fit to the correlation function obtained from *Magneticum* using

$$\xi_{sim}(r) = b^2 \xi_{model}(r \cdot \alpha) \tag{16}$$

where ξ_{sim} and ξ_{model} are the correlation function derived from *Magneticum* and the correlation function produced by our theoretical model, respectively, b is the ratio between the mean over density of galaxies to the mean over density of dark matter (i.e.

the *bias*), and α is a distance scaling factor. The b^2 factor is necessary because galaxy clustering does not exactly mirror the over densities in the bulk matter. A useful analogy would be that of "snow-capped mountains," where the altitude represents the dark matter density and the snow represents the galaxies. Only the tallest peaks are snow-capped with a strongly defined border to the snow. Meanwhile, the rest of the range is much more evenly distributed in mass with no defined borders even if there might be small peaks scattered about. In the same way that the snow does not completely reflect the topography of the ridge, galaxies do not completely reflect the overdensities in the bulk matter.

The scaling factor α enables adjustment of all length scales in the simulation to fit the model when the two involve different cosmological parameter values. Thus, α provides the key to inferring the correct cosmology. If $\alpha = 1$, then the cosmology used to create the models is the same as that of the observations. If, however, there is a discrepancy, the models will predict a different preferential separation distance (thus a different peak in ξ) than the data. We use that discrepancy to infer the correct cosmology for the data. As Eisenstein-Hu does not include a BAO peak, there is no reason to include a horizontal scaling factor α; therefore $\alpha \equiv 1$ for all Eisenstein-Hu fits.

We determine the fit paramerers α and β by minimizing χ^2, which is defined as follows

$$\chi^2 = \sum_{i=0}^{N} \sum_{j=0}^{N} \left(\Delta\xi(r_i)\right) C_{ij}^{-1} \left(\Delta\xi(r_j)\right), \tag{17}$$

where $\Delta\xi(r_k) = \xi(r_k) - \xi^m(r_k)$, $\xi(r_k)$ is the value of the correlation function of the simulation (i.e. *Magneticum*), $\xi^m(r_k)$ is the value of the correlation function at corresponding separations for a given model, and C is the covariance matrix between the correlation values at different length scales, r_i and r_j. Because a spatial resolution had to be chosen to create the correlation function, the normally continuous correlation function became incremental allowing us to index the separation distances.

Using the generated χ^2 matrix, the uncertainty in α was also calculated. Since α is the only value that we used in our analysis, we fixed b^2 to be the value at the minimum χ^2. We then calculated the two α values at which $\chi^2_r = 2(\chi^2_{r,min})$. This allowed us to obtain a 68% confidence interval in our α fit.

2.3 Extracting the Cosmological Parameters

At this point, the cosmology used to create the models is known, so D_V can be calculated for the four redshifts tested ($z = 0.20,\ 0.52,\ 0.72,\ \&\ 1.00$). The final D_V values for the data are the product of α and D_V^m resulting from the fiducial cosmology assumed in the models. That is, we can scale all lengths in the model (CAMB or EH) to match those in the simulation, thus finding the cosmology of the simulation. As such, the best-fit cosmology is the one that solves

$$\alpha \cdot D_V^m(0.272, 0.728) = D_V(\Omega_M, \Omega_\Lambda), \tag{18}$$

where D_V^m is the comoving volume distance of the *model*. Thus, since we are creating our initial models using WMAP values, $\Omega_M = 0.272, \Omega_\Lambda = 0.728$ for D_V^m. Had we created our models under a different cosmology (such as an Einstein-deSitter universe where $\Omega_M = 0, \Omega_\Lambda = 1$), then those would be the values present in Equation 18. We can find the best-fit cosmology by calculating D_V over a grid of Ω_M and Ω_Λ values using the simpler definition of χ^2 given below.

$$\chi^2 = \sum_{i=0}^{N} \left(\frac{\alpha \cdot D_V^m(z_i) - D_V(z_i)}{\Delta\alpha \cdot D_V(z_i)} \right)^2, \tag{19}$$

where $D_V^m(z_i)$ is the fiducial comoving volume distance and $D_V(z_i)$ is the comoving volume distance of the cosmology being tested.

Finally, the same method as before can be used to find the uncertainties on Ω_M

and Ω_Λ, and the fiducial cosmology can be compared with the best-fit cosmology. If the fiducial cosmology is within the error of the fit, there is promise for using correlation functions and the BAO to determine cosmological parameters.

3 Results & Discussion

The raw best-fit values of α, b^2, and χ^2 for each run and model are shown in Table 2.

One way to obtain a quantitative measure of the strength of the BAO peak is by the ratio of the χ^2 value of the best fit of Eisenstein-Hu as compared to that of CAMB, as shown in Figure 1. We can see that strength of the BAO peak behaves strikingly differently for galaxies and clusters. That is, the strength of the BAO evolves in the opposite sense for clusters and galaxies. For clusters, the ratio decreases as a function of redshift for all observations except $z = 1.00$, indicating that, on average, the BAO becomes less pronounced at larger redshifts. Contrarily, the strength of the BAO peak increases as a function of redshift for galaxy observations, except at the largest redshift as shown in Figure 8. These results can be seen in the correlation functions in Figures 2 through 17.

As shown in Table 3, $\alpha = 1$ is within the 68% uncertainty for all simulations, except for galaxies at $z = 0.52$. This is important because, in theory, α should be identically one as the same cosmology was used in the *Magneticum* data and the model. It is, therefore, expected that unity be within the errors of any calculated value.

Another important result of our analysis of the χ^2_r map is that α and b^2 are only weakly covariant. As an example, consider Figure 18, wherein a larger range of α and b^2 values are considered than in other samples. The most important feature is that the best fit value falls at the center of an egg-shaped contour plot. Secondly, this "egg" is vertically oriented, indicating that the fit parameters are independent. This

is fundamental to our ability to define meaningful errors on α without reference to the bias. We see that the error is around 10%, which is reasonable as an upper limit on observational precision. The local minimum around $\alpha = 0.7, b^2 = 0.4$ is negligible because it is unrealistic for $b^2 < 1$, as this would imply that galaxies are more over dense than dark matter, which only occurs on very small scales (less than 10 Mpc/h) (Myers et al. 2005).

Knowing that we can consider α independently from the bias, we calculated $D_V(z)$, which is plotted in Figure 19, where the best fit cosmology is $\Omega_M = 0.350$ and $\Omega_\Lambda = 1.00$ for galaxies and $\Omega_M = 0.340$ and $\Omega_\Lambda = 1.00$ for clusters. We also create maps of probabilities for any given cosmology. Figure 20 shows the probability space for galaxies and Figure 21 gives the data for clusters. The ellipses represent the space for 68%, 95%, and 99.5% confidence intervals. The diagonal dotted line runnning from the upper left to the lower right represents possible cosmologies for a flat universe. The white point represents the fiducial WMAP-7 cosmology.

We can see that the correct cosmology is near the 68% confidence interval of the best-fit calculation for both galaxies and clusters. However, the 68% confidence interval is extremely large, indicating that something in our model needs to be more constricted for this method to be useful.

We believe the source of the unreasonably large uncertainty stems from the size of our sample. The data herein were created such that there were on the order of 10^6 objects in the sample, with fewer objects as we look further back in time. We believe that the number of objects in the random sample determines these uncertainties, and so increasing the number of objects in the simulation should decrease the uncertainties.

The number of objects in the sample also affects the noise in the correlation function itself. We saw that at large redshifts, the correlation function becomes very erratic, while still following the general shape of the BAO. This is most likely due

to the fact that there are simply not enough clusters in our sample to overcome this noise. So, a larger sample volume would also smooth the correlation function at high redshifts. Increasing the sample size also brings the simulation more in accord with the potential *Euclid* data, which is projected to measure photometric redshifts of over 50 million objects. (Laureijs et al. 2011)

There is also a dependence of signal detection on distance. Using $R(\chi^2)$ as our metric, Figure 16 shows the most well-defined BAO peak, which occurs at $z = 1.00$, while Figure 2 shows the least well-defined BAO peak, which occurs at $z = 0.20$. In the high redshift case, it is both visually and mathematically clear where the BAO peak is. In the low redshift correlation function, however, it is much less clear: does the peak span 90 to 100 Mpc/h or is it the single bump at $r \approx 103$ Mpc/h? This, we expect, is the cause of the large α values at low redshifts, and thus the resulting extreme Ω_Λ values.

4 Conclusions

We sought to develop a method to constrain Ω_M and Ω_Λ using the peak in the correlation function caused by BAO. Using *Magneticum*, a smooth particle hydrodynamic simulation, we created eight correlation functions using both galaxies and clusters of galaxies as our tracers at four different redshifts. We fit those functions with theoretical models centered around the Baryon Acoustic Oscillation peak to obtain two fit parameters, α, which is a horizontal scaling factor, and b^2, which is a vertical scaling factor associated with the bias. Using α, we found the cosmology that best replicated the comoving volume distance associated with our data. We found that we can reproduce the correct cosmology with 68% confidence using both galaxies and clusters of galaxies, although the best-fit cosmology ($\Omega_M = 0.350, \Omega_\Lambda = 1.00$ for galaxies and $\Omega_M = 0.340, \Omega_\Lambda = 1.00$ for clusters) is far from the fiducial cosmology of WMAP7

($\Omega_M = 0.272, \Omega_\Lambda = 0.728$). We see that the strength of the BAO signal (measured by $R(\chi^2)$, the ratio of the goodness of fit of the Eisenstein-Hu model divided by that of the CAMB model) is roughly dependent on the redshift of the observation, with higher redshifts corresponding to stronger signals. We also see, however, that the smoothness of the signal deteriorates with redshift, causing cluster correlation functions to become very noisy. These results suggest that a larger sample volume is critical to the potential success of this method to usefully constrain Ω_M and Ω_Λ.

Further tests of this method have begun where the *Magneticum* volume is 19.4 $(Gpc/h)^3$, or 27 times the volume of the current simulation. Such a large data set provides many opportunities to assess the detailed application of this model, but also provides a number of challenges, some of which are still being addressed. The first of these difficulties is the sheer number of objects. The run time of the calculation of the correlation function is in $O(N^2)$. As such, we must artificially limit the number of objects being considered in our analysis given our computational restrictions. The most reasonable method to accomplish this is via a cut-off of objects above some minimum mass. We chose a minimum mass of the tracer such that there are around one million objects in our sample. Altering the lower mass limit to maintain one million objects also ensures that the statistical significance of the results do not depend on extrinsic factors such as the number of objects. In order to accomplish this, we calculate the number of galaxies in the sample with mass greater than each given mass, as shown in Figure 22.

After this, our analysis method continues as before. However, the correlation plots which result from this simulation are peculiar when compared to those of the smaller-volume simulation as exemplified in Figure 23. In fact, the correlation function is much more erratic in its shape with unreasonably small error bars. As we are not yet able to explain this strange behavior in the data, we do not plan to extract the cosmological parameters for this new simulation until the correlation function can be

justified.

Overall, the theory behind constraining the cosmological parameters using the correlation function is sound, but there are still many functional hurdles to overcome before the method can be expected to produce significant results. Both the precision and the accuracy need significant improvements in order to reflect the input parameters of *Magneticum*. We believe this can be accomplished using larger sample volumes if internal inconsistencies can be accounted for. If this occurs, then we look forward to applying this new geometry-based method to the *Euclid* data in the near future to further restrict the values of Ω_M and Ω_Λ.

5 Acknowledgments

Thank you to the Union College Summer Research fund for providing me with the financial resources to begin this research. Thank you to Lauro Moscardini, Federico Marulli, and Alfonso Veropalumbo from the University of Bologna for their help and guidance throughout this work. Jon Marr as well has been a fantastic advisor, providing support and guidance me in interpreting and analyzing the data. Thank you to Greg Hallenbeck for his invaluable aid in learning the statistics necessary to analyze this data. And finally, thank you to the Union College Department of Physics and Astronomy for providing me with the opportunity to conduct a senior thesis, as well as for supporting me in my academic endeavors throughout my undergraduate career.

References

Alpher, R.A., Bethe, H., & Gamow, G., 1948, Phys. Rev., 73, 803-804

Blake, C. & Glazebrook, K. 2003, ApJ, 594, 665

Dolag A. et. al., in preparation

Dolag K., Vazza F., Brunnetti G., & Tormen G., 2005 MNRAS, 364, 753

Eisenstein D. et al., 2005 ApJ, 633, 560

Eisenstein D. & Hu W., 1998 ApJ, 496, 605

Friedmann, A. 1922, Zeitschrift fur Physik, 10, 377

Guth, A. H. 1981, Phy. Rev. D, 23, 347

Hogg, D. W., 2000 arXiv:astro-ph/9905116

Hubble, E. 1929, PNAS, 15, 168

Komatsu, E., Smith, K. M., Dunkley, J., et al. 2011, ApJS, 192, 18

Landy, S. D., & Szalay, A. S. 1993, ApJ, 412, 64

Laureijs, R., Amiaux, J., Arduini, S., et al. 2011, arXiv:1110.3193

Lewis A., & Bridle S., 2002, Phys. Rev. D, 66, 103511

Mather, J. C., Cheng, E. S., Eplee, R. E., Jr., et al. 1990, ApJ Letters, 354, L37

Myers, A. D., Outram, P. J., Shanks, T., et al. 2005, MNRAS, 359, 741

Peebles P. J. E., 1993, Principles of Physical Cosmology, Princeton University Press, Princeton

Peebles, P. J. E. 1980, The Large-Scale Structure of the Universe, Princeton University Press, Princeton

Peebles, P. J. E. & Yu, J. T. 1970, ApJ, 162, 815

Penzias, A. A., & Wilson, R. W. 1965, ApJ, 142, 419

Riess, A. G., et al. 1998, AJ, 116, 1009

Ryden, B., 2002, Introduction to Cosmology (San Francisco: Addison-Wesley)

Springel V., et al., 2005, Nature, 435, 629

Table 1. Current Accepted Values of Cosmological Parameters. All results taken from (Komatsu et al. 2011)

Parameter	Description	Value
H_0	Hubble Constant	$70.4^{+1.3}_{-1.4}$ km/s/Mpc
t_0	Age of the Universe	13.75 ± 0.11 Gyr
Ω	Total Density Parameter	$1.0023^{+0.0056}_{-0.0054}$
Ω_M	Total Matter Density	0.272
Ω_{BM}	Baryon Density	0.046 ± 0.002
Ω_{DM}	Dark Matter Density	0.227 ± 0.014
Ω_Λ	Dark Energy Density	$0.728^{+0.015}_{-0.016}$

Table 2. Best Fit Parameters for all ξ. Note that $\alpha \equiv 1$ for all EH models.

Tracer	Redshift	Model	$\bar{\chi}^2$	α	b^2
galaxy	0.20	CAMB	17.589	1.101	1.986
galaxy	0.20	EH	20.879	–	1.773
galaxy	0.52	CAMB	22.412	1.083	3.630
galaxy	0.52	EH	27.972	–	2.659
galaxy	0.72	CAMB	13.026	1.008	2.962
galaxy	0.72	EH	19.722	–	2.342
galaxy	1.00	CAMB	5.687	1.029	3.647
galaxy	1.00	EH	7.356	–	3.433
cluster	0.20	CAMB	1.415	1.026	1.613
cluster	0.20	EH	2.193	–	1.293
cluster	0.52	CAMB	0.771	1.090	1.840
cluster	0.52	EH	1.049	–	1.330
cluster	0.72	CAMB	1.117	1.032	2.652
cluster	0.72	EH	1.44	–	2.342
cluster	1.00	CAMB	0.904	1.056	3.576
cluster	1.00	EH	1.564	–	1.644

Table 3. Best Fit α Values and Associated Uncertainties for the CAMB Model

Tracer	Redshift	α	$-\Delta\alpha$	$\Delta\alpha$
galaxy	0.20	1.101	0.177	0.078
galaxy	0.52	1.083	0.063	0.045
galaxy	0.72	1.008	0.108	0.120
galaxy	1.00	1.029	0.072	0.105
cluster	0.20	1.026	0.075	0.102
cluster	0.52	1.090	0.130	0.180
cluster	0.72	1.032	0.093	0.141
cluster	1.00	1.056	0.084	0.099

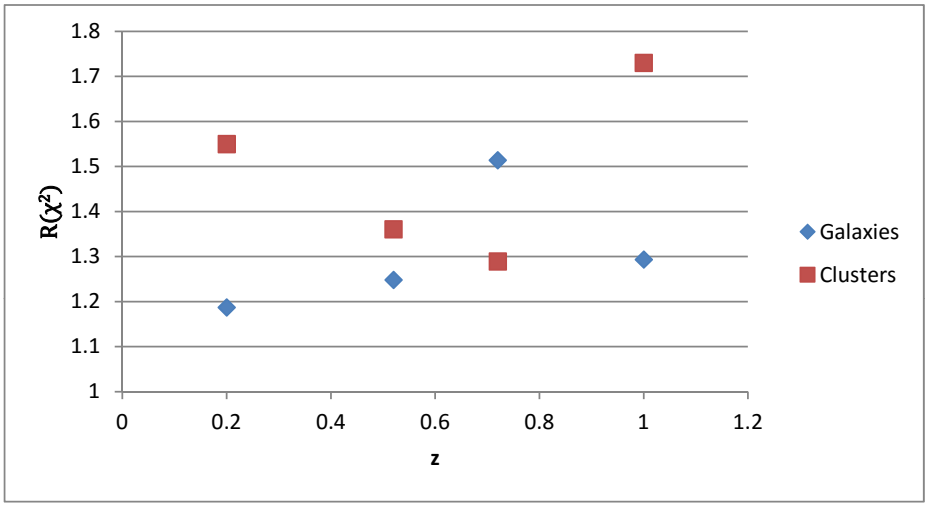

Figure 1: The ratio of the best fit χ^2_r for the Eisenstein-Hu model compared to that of the CAMB model, denoted $R(\chi^2)$. Notice that for clusters, the ratio of the goodness of fit decreases excluding the measurements at $z = 1.00$. This is the complete opposite of the results for galaxies, where EH has a decreasing goodness of fit relative to CAMB for all by the last observation.

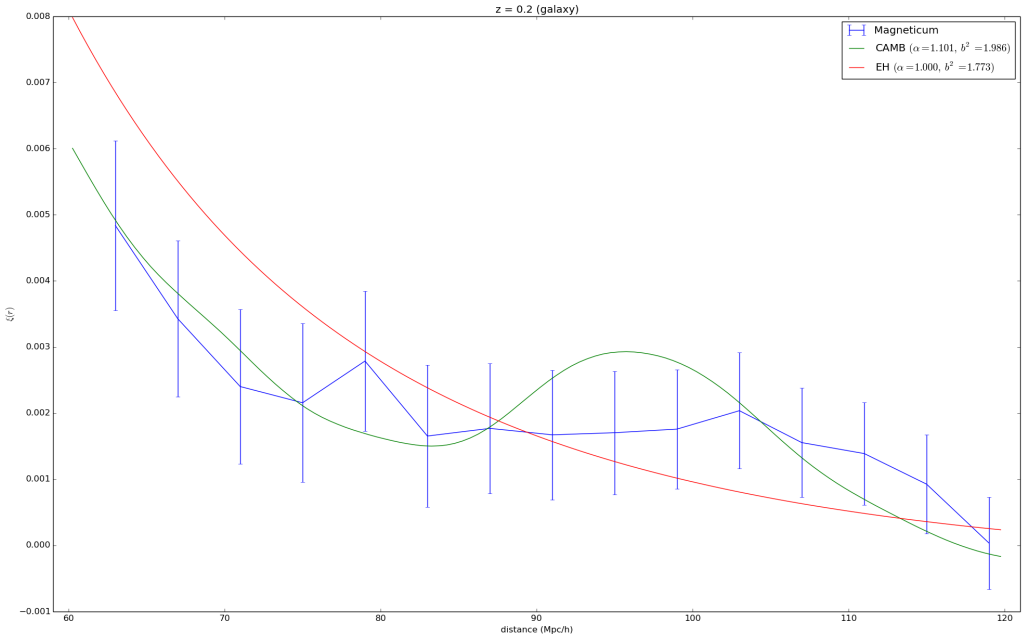

Figure 2: Correlation function at $z = 0.2$ for galaxies in the *Magneticum* Simulation (blue), CAMB (green), and EH (red). At low redshifts, the BAO peak is very weak. The signal at 78 Mpc/h is not associated with the BAO and is of unknown origin.

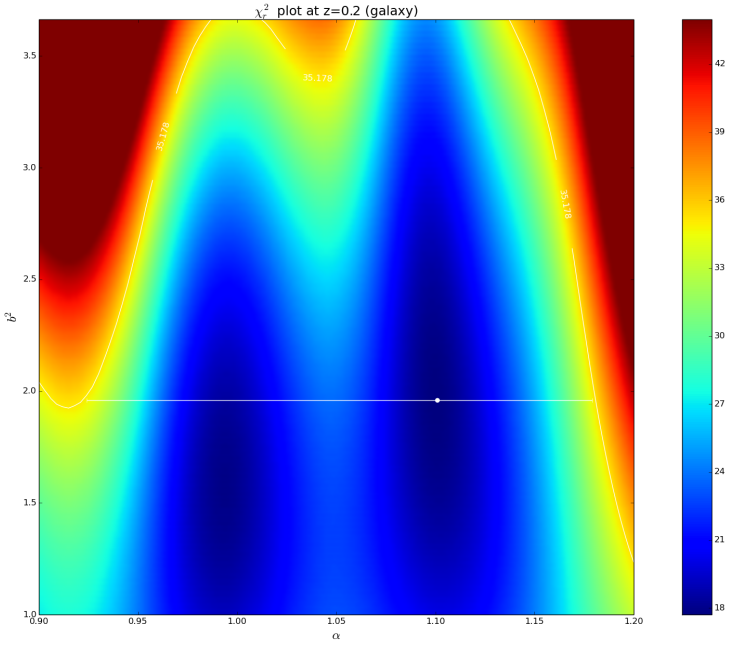

Figure 3: Notice that there are two minima in the reduced chi squared. Although the minimum around $\alpha = 1$, is the preferable choice, χ_r^2 is smaller at the minimum at $\alpha \approx 1.1$.

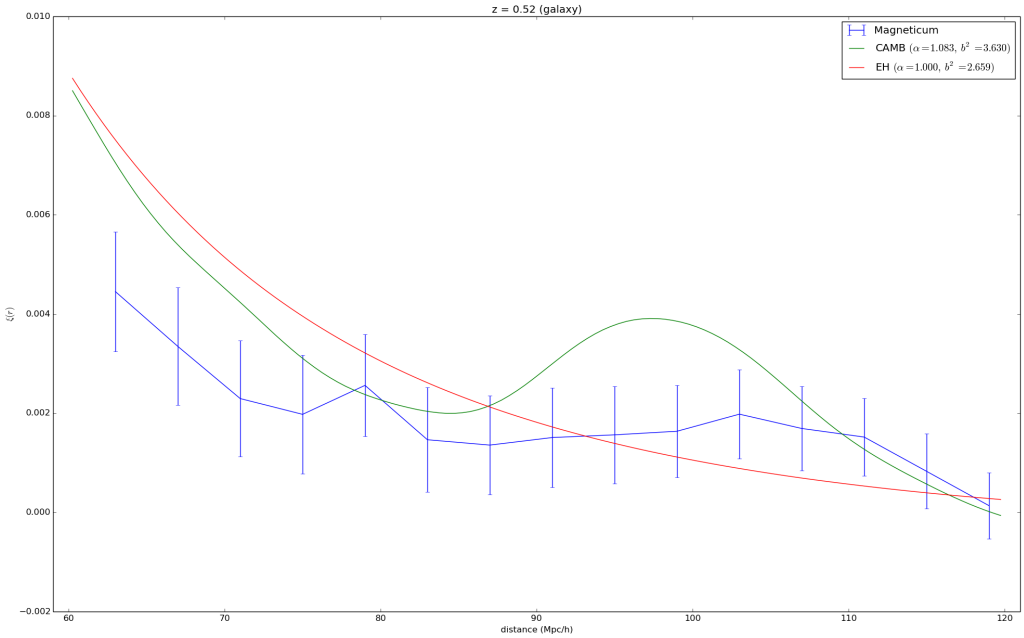

Figure 4: Correlation function at $z = 0.52$ for galaxies. The BAO peak is beginning to appear in the correlation function, but still can be explained as a noise peak.

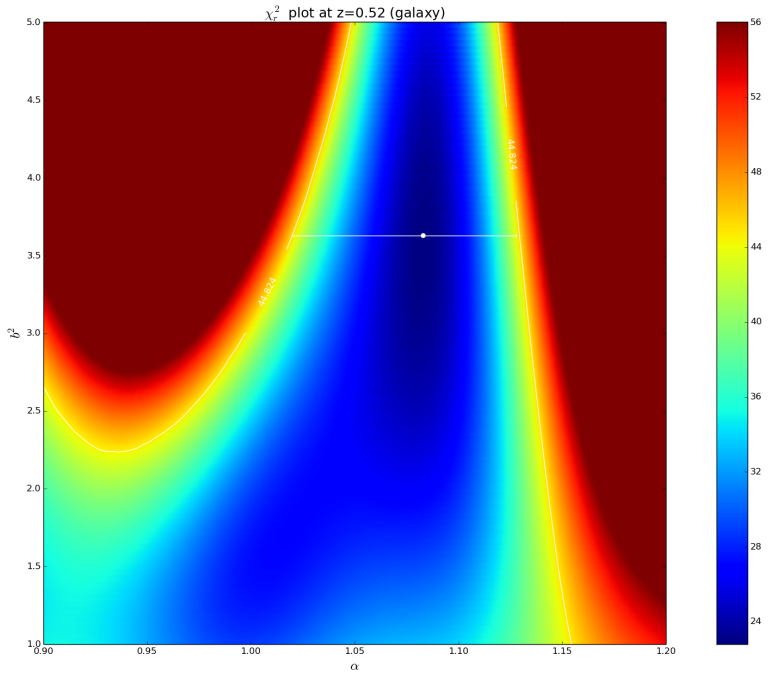

Figure 5: Because the correlation function is still very flat, there is a large range of bias values which fit the data reasonably well.

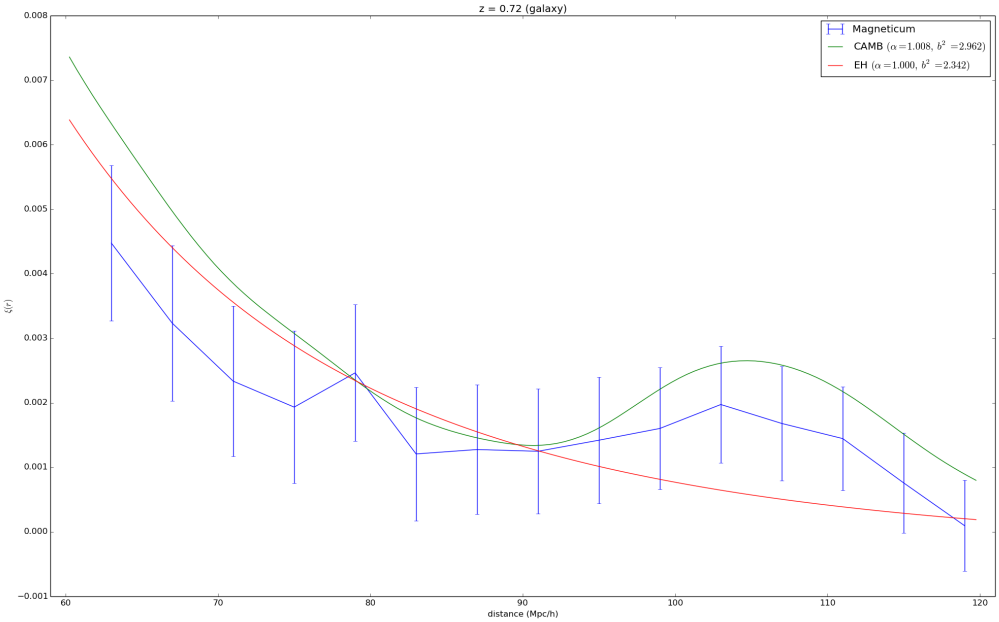

Figure 6: Correlation function at $z = 0.72$ for galaxies. Here, we have the first verifiable trace of the BAO peak in the correlation function. As such, the best fit scale parameters now match visual expectations much more strongly.

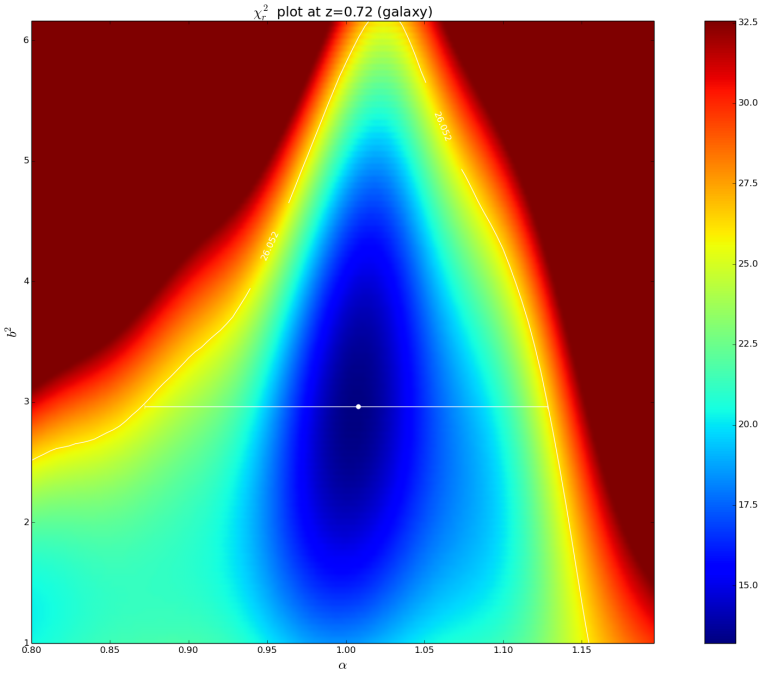

Figure 7: The minimum χ_r^2 is now much lower than previous samples. We also see that the range of reasonable fit parameters is starting to shrink.

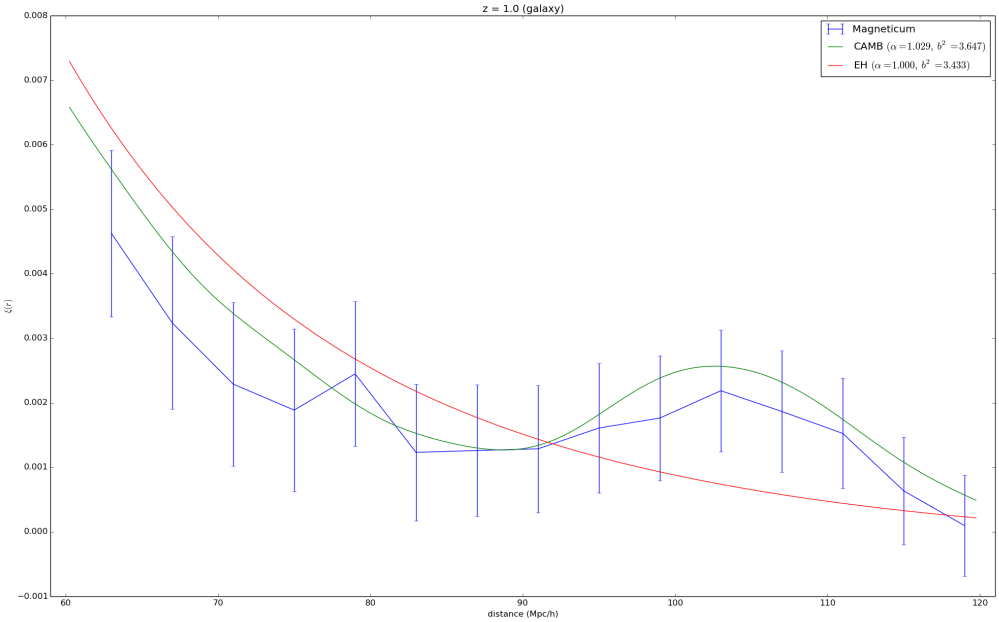

Figure 8: Correlation function at $z = 1.0$ for galaxies. At the largest redshift analyzed, the BAO peak is very well defined. We see that CAMB well predicts the correlation function from *Magneticum*, and the Eisenstein-Hu model does a poor job of fitting the function.

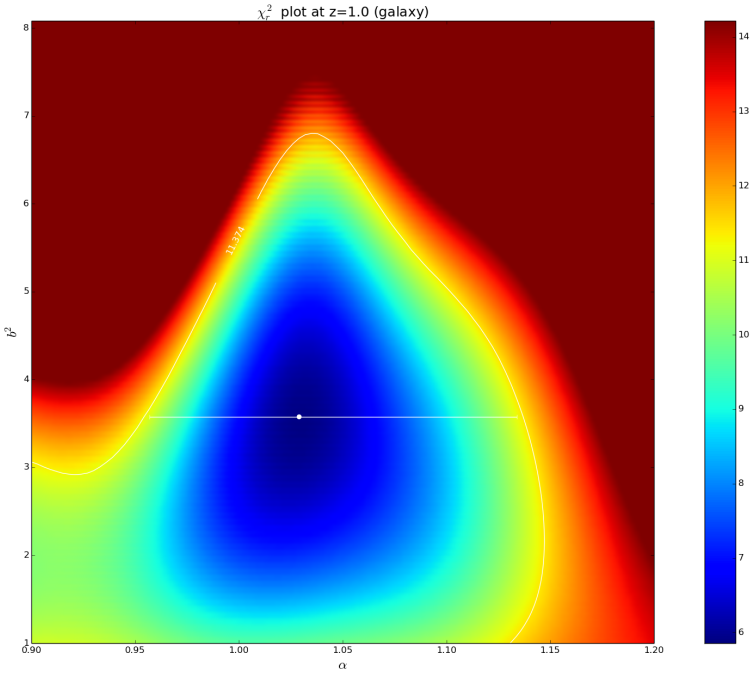

Figure 9: Although the range of acceptable α is larger, the minimum χ_r^2 is much smaller than any other observation with galaxies.

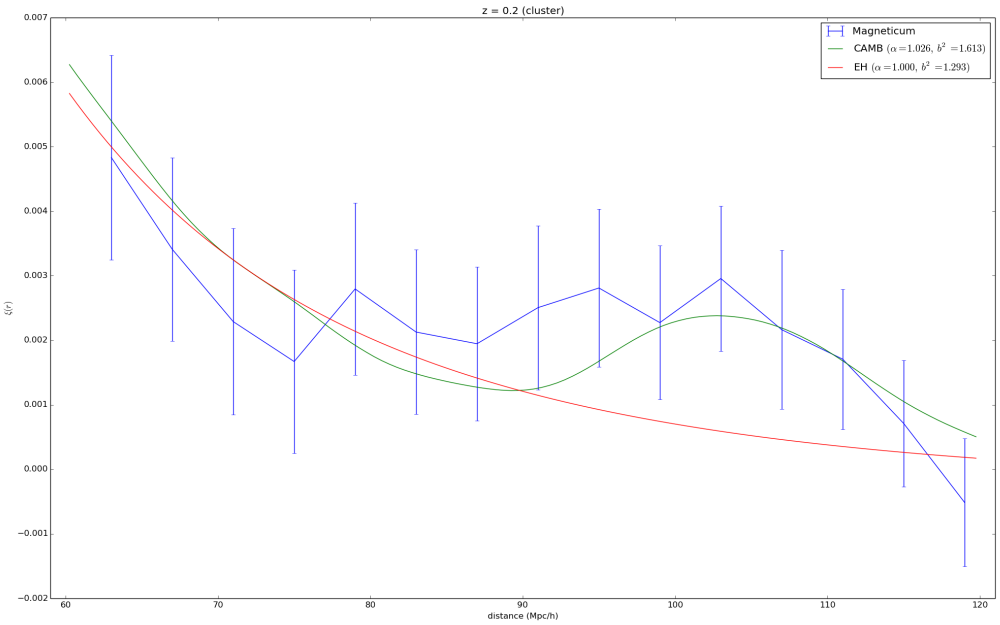

Figure 10: Correlation function at $z = 0.2$ for clusters. Even at low redshift, the correlation function of clusters has a broad peak due to the BAO. However, there is also significantly more noise in the signal, which will only get worse.

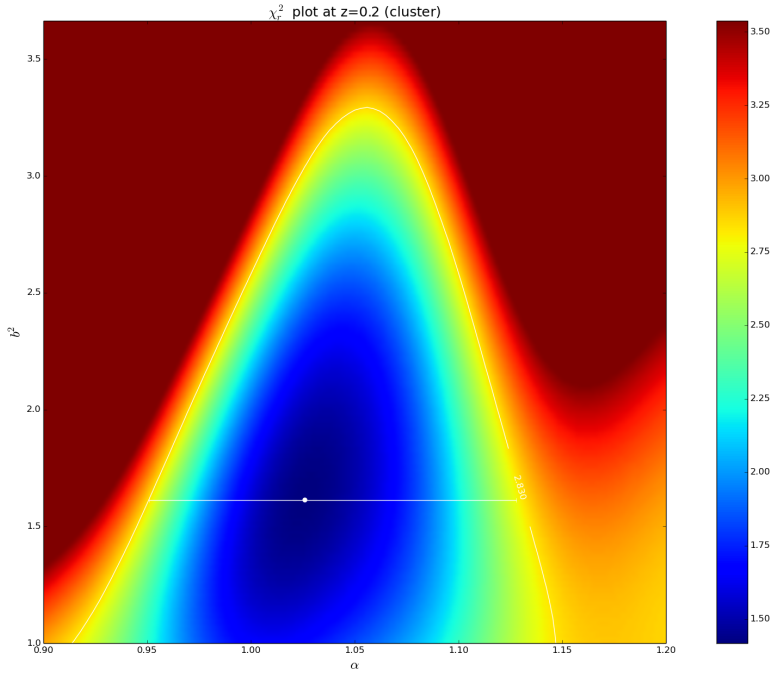

Figure 11: Cluster correlation functions are much more in accordance with prediction, which is evident from the fact that the minimum χ_r^2 is around one.

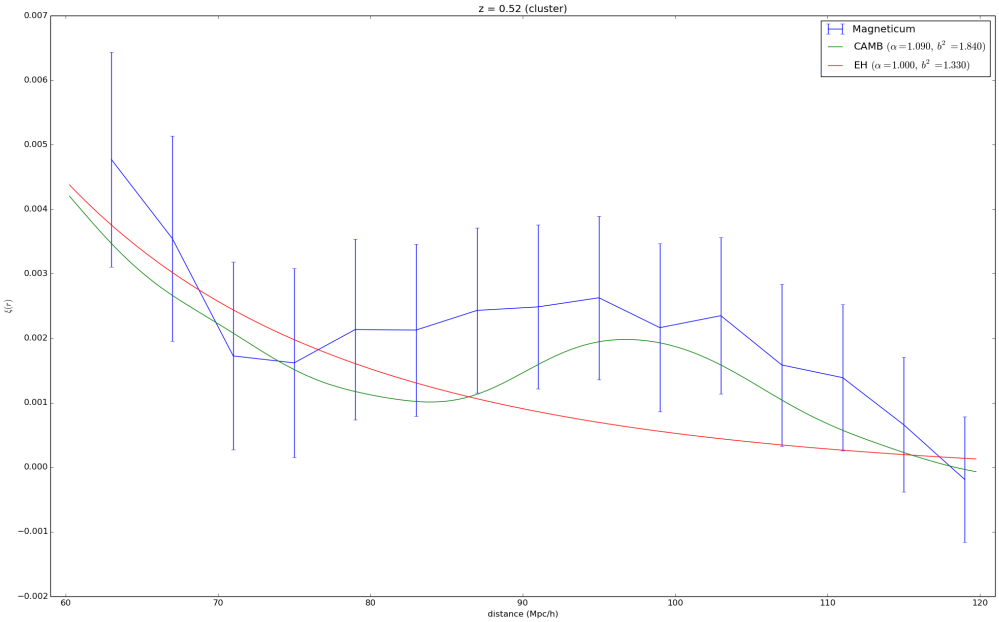

Figure 12: Correlation function at $z = 0.52$ for clusters. The BAO peak is still very broad likely due to the fact that this is still a low redshift observation.

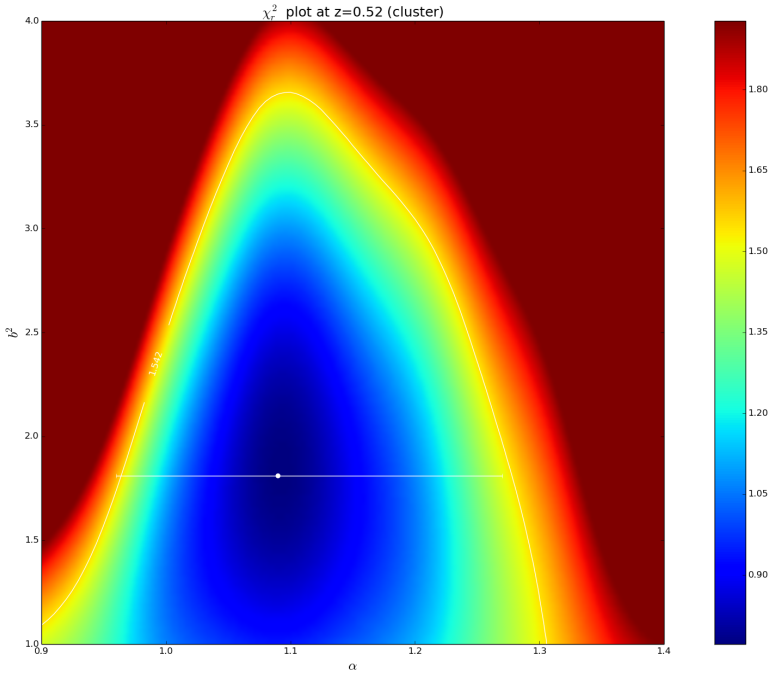

Figure 13: The reduced chi squared shows that there is a large range of fit parameters within 68% of the minimum, but this range is a much better fit than most of those for galaxy observations.

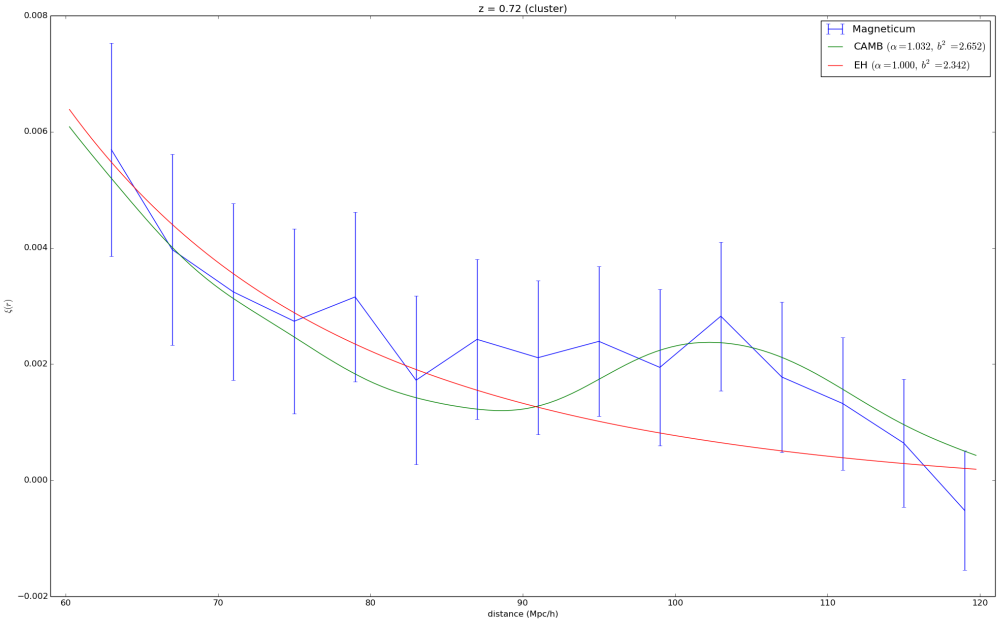

Figure 14: Correlation function at $z = 0.72$ for clusters. The correlation function is becoming very noisy at larger redshift, which is likely due to under-sampling as *Magneticum* is volume-limited.

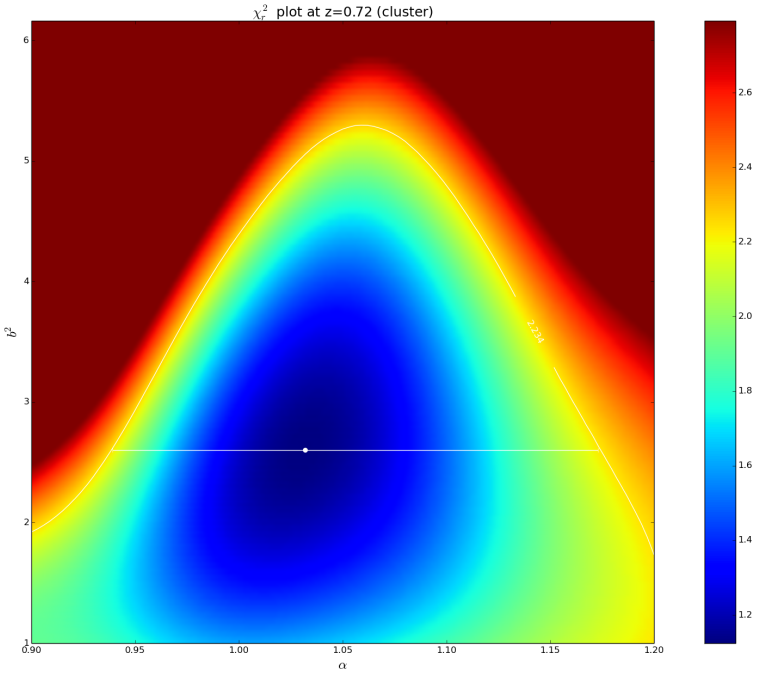

Figure 15: With the increase in noise, the range of acceptable fit parameters becomes even larger.

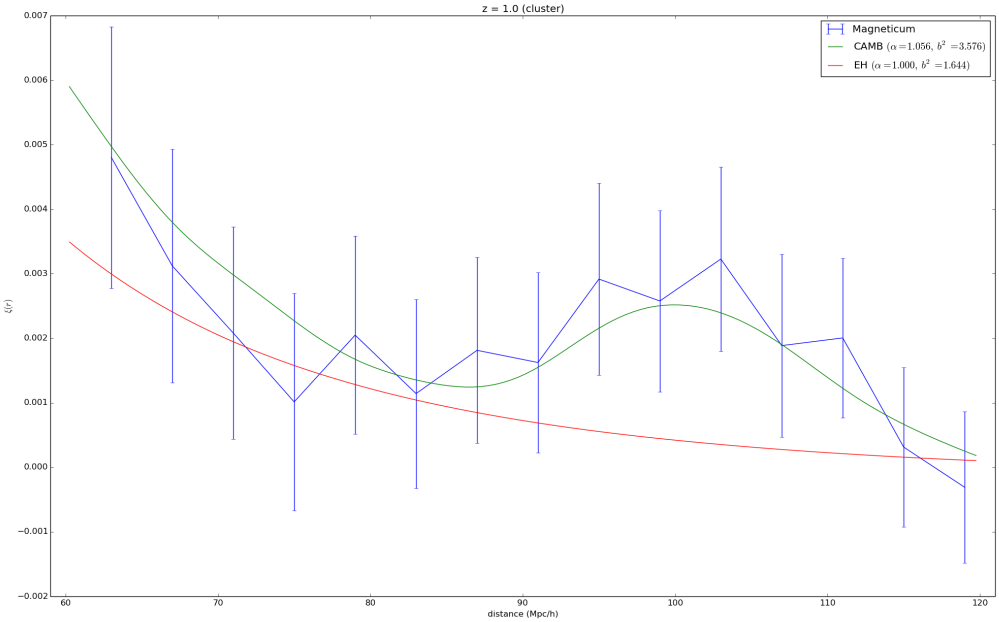

Figure 16: Correlation function at $z = 1.0$ for clusters. At the largest redshift considered, the BAO peak is very well defined (and well modeled), even though the signal is beginning to degenerate due to under sampling.

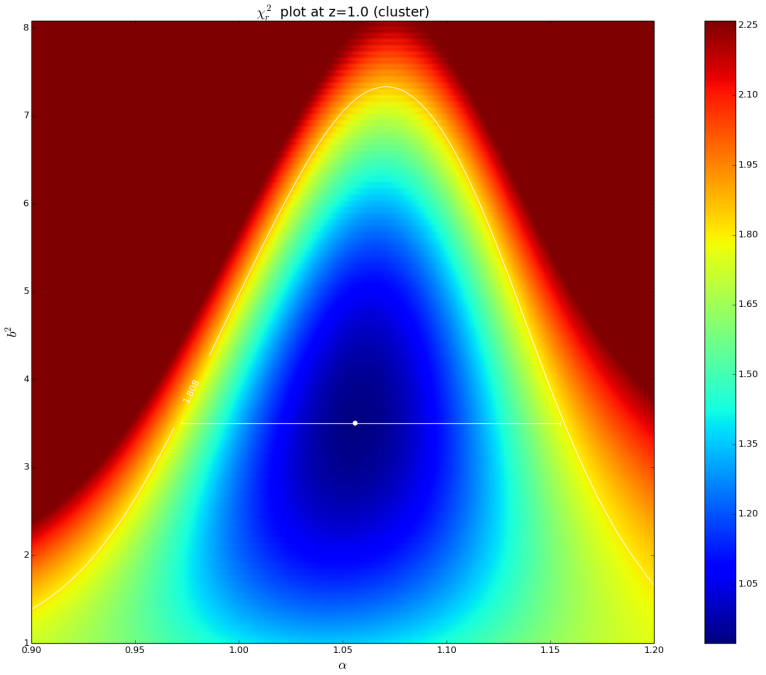

Figure 17: Even with all of the noise in the correlation function itself, the goodness of fit is not strongly affected.

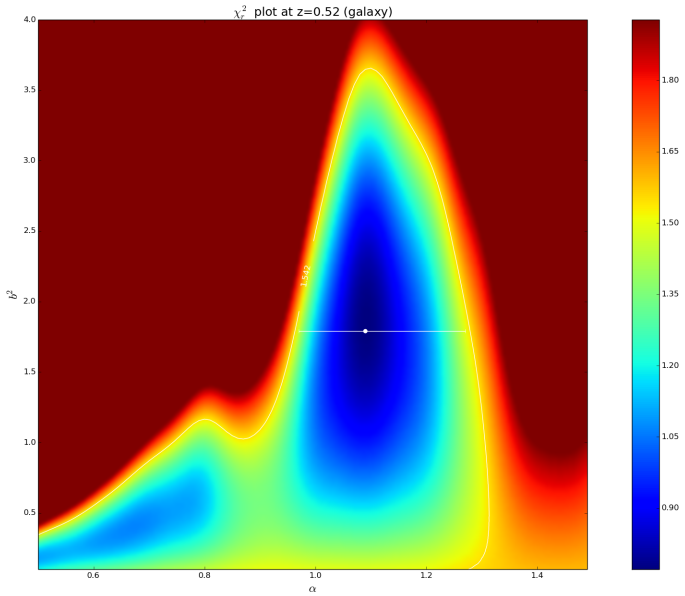

Figure 18: A plot of χ_r^2 over a larger range than normally considered using clusters as the tracer at $z = 0.52$. Notice that the contour lines are vertically oriented, implying that α and b^2 are independent, allowing us to consider the uncertainty in α without concern for the bias.

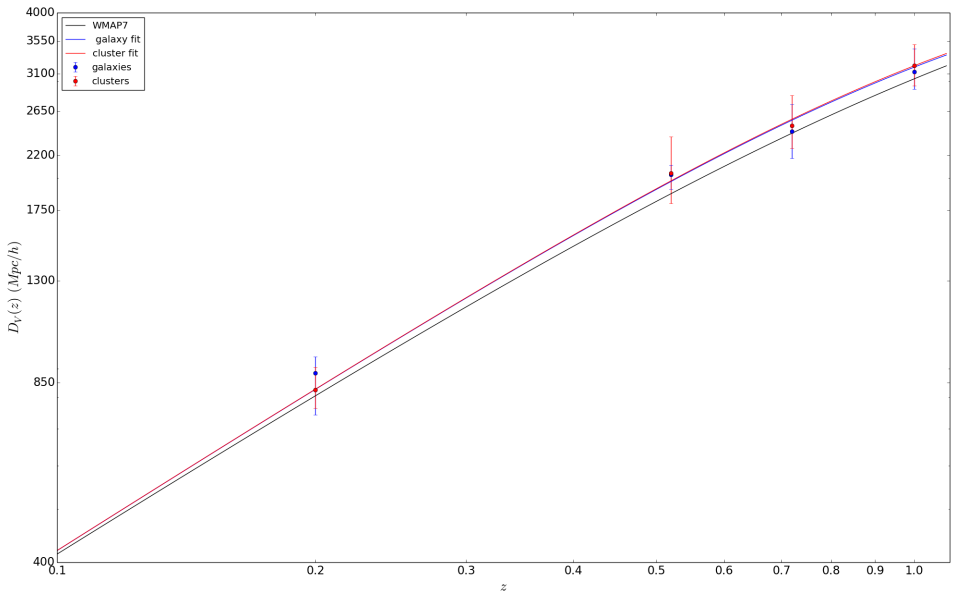

Figure 19: Notice that the $D_V(z)$ values are all larger than that due to the fiducial cosmology as all $\alpha > 1$. This pulls the best fit cosmology upward, which requires $\Omega_M = 0.34$ and $\Omega_\Lambda = 1.00$.

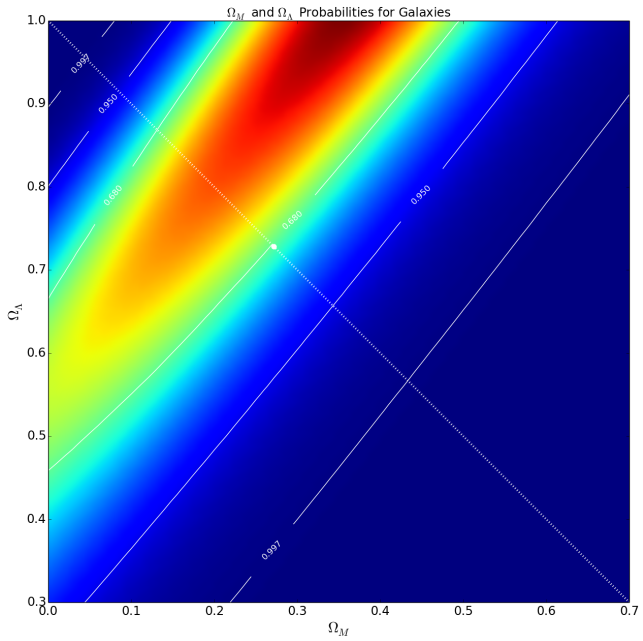

Figure 20: The actual cosmology used to create the data, given by the white point, is right on the edge of the 68% confidence interval. Surprisingly, the best fit cosmology requires $\Omega_\Lambda = 1.00$.

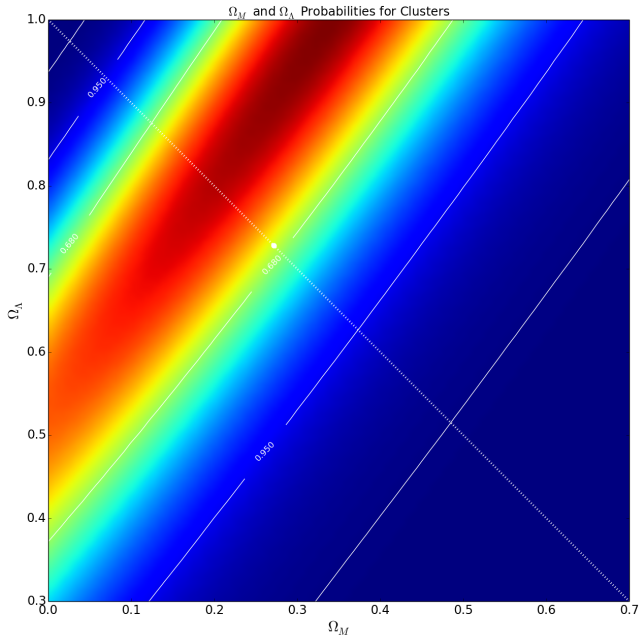

Figure 21: The actual cosmology used to create the data is within the 68% confidence interval, although said interval is quite large. Again, the best fit cosmology requires $\Omega_\Lambda = 1.00$.

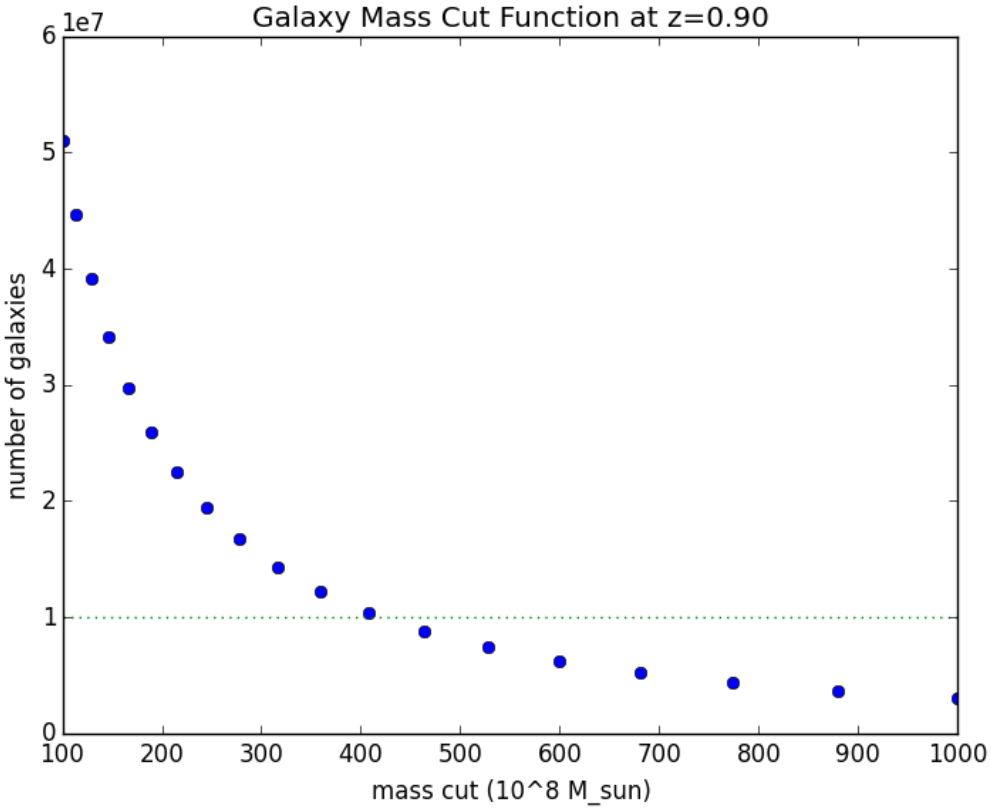

Figure 22: Requiring an object to be at least $4 \times 10^{10} M_{\odot}$ (approximately the size of the Large Magellanic Cloud) to be considered a galaxy allows us to have approximately one million objects in our galaxy sample. We see that as we go to smaller masses, the slope increases, indicating that that are more less massive objects in our sample than massive objects.

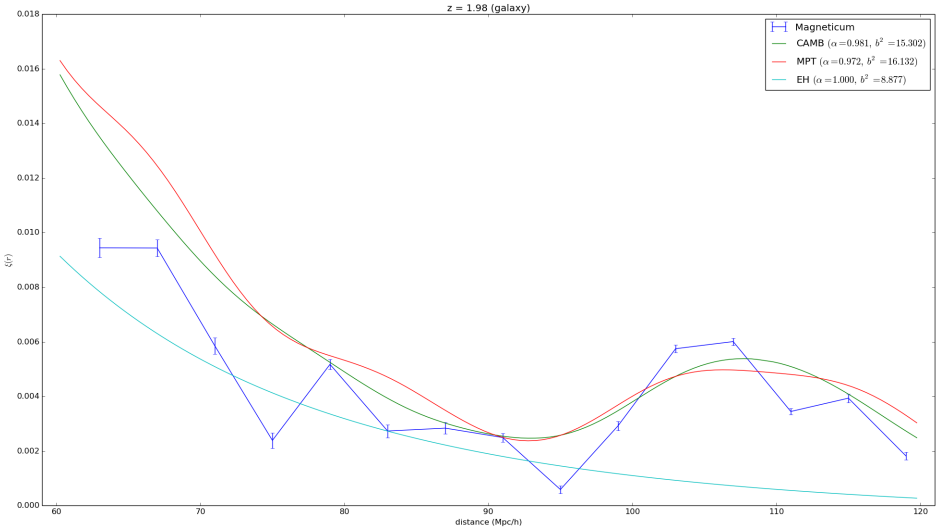

Figure 23: The correlation function at $z = 1.98$ created using the larger-volume sample does have significantly smaller inherent uncertainties, but the function itself is so erratic that no meaningful analysis can be extracted.